

# Prospects of $A$ and $Z$ identification experiments at LBNL

Jacklyn M. Gates<sup>a</sup>

Lawrence Berkeley National Laboratory, Berkeley, CA 94720, USA

**Abstract.** The identification of six new elements within the last 15 years and with proton numbers,  $Z = 113$ – $118$  has transformed the heavy element field. However, one key piece of information on these nuclei remains unmeasured: their proton and mass numbers,  $A$ . At Lawrence Berkeley National Laboratory, the heavy element group has undertaken a program to study these new elements to perform experiments aimed at measuring the  $Z$  and  $A$ . Here, an overview of recent experiments aimed towards identifying the  $Z$  of SHE, and the prospects for  $Z$  and  $A$  identification experiments at LBNL are presented.

## 1. Introduction

Over the last 15 years, multiple experiments have been performed to produce elements with proton numbers,  $Z = 113$ – $118$  at the Flerov Laboratory for Nuclear Reactions using reactions of  $^{48}\text{Ca}$  on actinide targets [1]. Many of these experiments have been successfully reproduced at laboratories around the world [2–8]. Several of the new nuclei have been produced in multiple reactions, i.e.  $^{283}112$ , produced directly in the  $^{238}\text{U}(^{48}\text{Ca},3n)$  reaction and as a (grand)daughter nucleus in the  $^{242}\text{Pu}(^{48}\text{Ca},3n)$ ,  $^{244}\text{Pu}(^{48}\text{Ca},5n)$  and  $^{245}\text{Cm}(^{48}\text{Ca},2n)$  reactions [9–11]. Taken together, the experiments present a self-consistent set of data regarding the production and decay properties of these new nuclei, hereafter referred to as Superheavy Nuclei (SHE). While no measurement of  $Z$  or link to nuclei with known  $Z$  has been made, the new nuclei have been assigned to elements with  $Z = 113$ – $118$  based on the large amount of data from cross bombardments and excitation function measurements [12, 13].

While there is little reason to doubt the assigned proton numbers, a direct measurement of SHE  $Z$  and mass numbers,  $A$ , is of great interest. Presently, there are three main ways to determine  $Z$  and  $A$  of SHE: (i)  $A$  and  $Z$  determination by linking to known elements, (ii)  $Z$  determination through the observation of characteristic  $Kx$ -rays, and (iii)  $A$  determination through mass measurements. At Lawrence Berkeley National Laboratory (LBNL) we are currently working on methods (ii) and (iii) for further investigating SHE. Here an overview of recent experiments aimed towards identifying the  $Z$  of SHE, and the prospects for  $Z$  and  $A$  identification experiments at LBNL are presented.

---

<sup>a</sup> e-mail: jmgates@lbl.gov

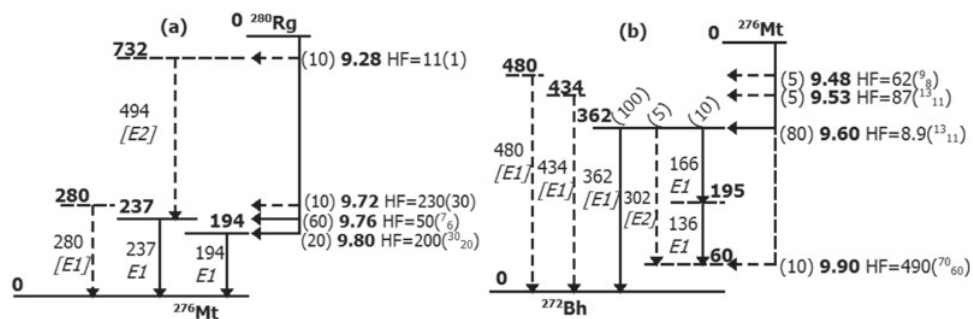


**Figure 1.** Proposed level schemes for  $^{276}\text{Mt}$  ( $Z = 109$ ) and  $^{272}\text{Bh}$  ( $Z = 107$ ), adapted from [7].

## 2. Prospects for Z identification experiments at LBNL

At Lawrence Berkeley National Laboratory (LBNL), separation of evaporation residues (EVRs) of interest from unwanted background is achieved using the Berkeley Gas-filled Separator (BGS) [14]. The BGS couples high EVR efficiency with high separation factors, which has allowed for the study of nuclides produced at rates of atom-per-day to atom-per-month [2, 7, 8, 15] in recent years. At the focal plane of the BGS is the corner-cube-clover (C3) detector, which consists of three double-sided silicon-strip detectors (DSSD) in the shape of the corner of a cube, and three high-purity germanium clover-type detectors (HPGe) press up against the face of each DSSD [7, 15]. The combination of DSSDs and HPGe allows for the detection of  $\gamma$ - and  $x$  rays emitted with the decay of SHE. The C3 detector has been discussed before and has a measured full energy  $\alpha$ -particle detection efficiency of 77(5)% and a maximum photon efficiency of 30(2)% for  $E_{ph} = 120$  keV [7].

### 2.1 Attempt using the $^{243}\text{Am}(^{48}\text{Ca}, xn)^{291-x}115$ reaction

The  $^{243}\text{Am}(^{48}\text{Ca}, xn)$  experiment was performed in 2013 and previously published [7]. During the experiment, 46 decay chains were observed that could be attributed to the decay of element 115. Forty-three of the decay chains were “long” chains consisting of EVR- $\alpha$ - $\alpha$ - $\alpha$ - $\alpha$ -SF decay chain while the other three chains were short EVR- $\alpha$ -( $\alpha$ )-SF chains. All 46 decay chains were attributed to the decay of  $^{288}115$  based on the observed decay properties [16, 17].

Over the course of the experiment, multiple  $\alpha$ -photon coincidences were observed with the decay of  $^{280}111$  and  $^{276}109$  allowing for level schemes for the low-lying levels above  $^{276}109$  and  $^{272}107$  to be devised. The level schemes are reproduced here in Fig. 1. Unfortunately, no SHE Z identification could be made based on the observed data.

## 3. Prospects for A identification experiments at LBNL

Without a definitive Z identification in the  $^{243}\text{Am}(^{48}\text{Ca}, xn)$  reaction, the focus at LBNL has shifted to determining the A of a SHE. While the BGS, has a high efficiency and great suppression of beam and unwanted reaction products, these come at a cost: the BGS has a mass resolution of  $A/\Delta A \sim 20$ , a relatively large focal plane image [14], and the detector station is in a high neutron and  $\gamma$ -ray background region. Currently, the BGS is being upgraded to couple to the mass analyzer, FIONA (For the Identification Of Nuclide A).

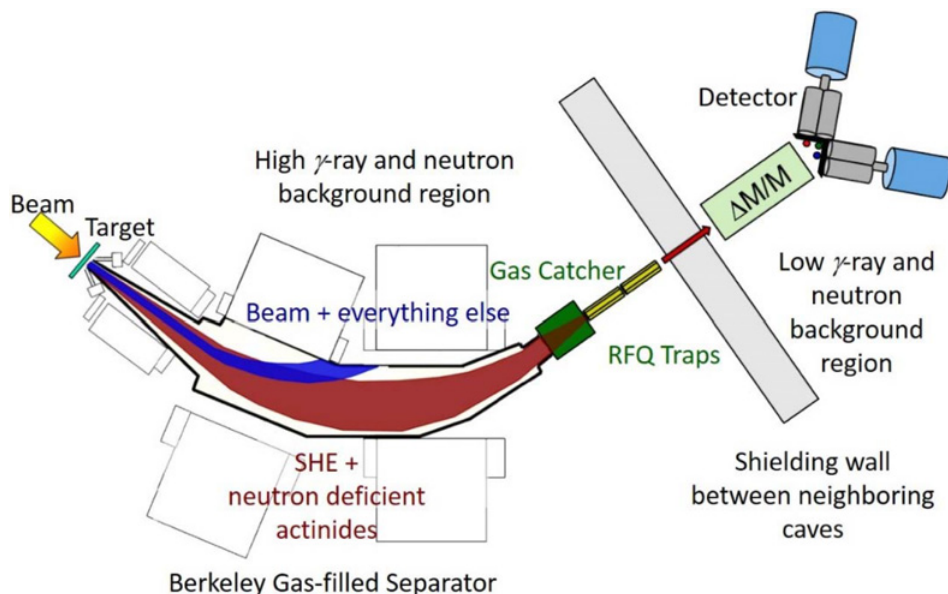


**Figure 2.** Basic schematic of the new BGS + FIONA apparatus in LBNL. See text for details.

A basic schematic of the setup is shown in Fig. 2. The goal of the upgrade is to provide a low energy, mass separated “beam” of SHE to a low neutron and  $\gamma$ -ray background region for  $A$  identification and nuclear structure studies, which includes  $Z$  identification through  $K\alpha$  ray observation.

Coupling the mass analyzer to the BGS is done using a technique that has been employed with setups such as CARIBU at Argonne National Laboratory [18], and SHIPTRAP at the GSI [19, 20]. The EVRs are thermalized in a radiofrequency (RF) gas catcher at the BGS focal plane, cooled and bunched in a radiofrequency quadrupole (RFQ) trap and then re-accelerated through a shielding wall and into a neighbouring cave, where they are separated by mass. By having the mass analyzer in a separate cave from the BGS, we can study the transmitted EVRs in a low neutron and  $\gamma$ -ray background region.

The gas catcher, RFQ traps and acceleration were developed and built at Argonne National Laboratory (ANL), while LBNL designed the mass analyzer. There were several requirements to take in account in the design of the mass analyzer:

- $A/\Delta A \geq 300$  – with production rates of atoms-per-day, mass determination should require the observation of only three atoms.
- High dispersion – the pixelation on the BGS focal plane detector is  $2 \times 2$  mm, therefore, adjacent masses should be separated by about one centimeter.
- Low extraction voltage from RFQ and acceleration across a gap of  $<10$  kV.
- High efficiency – the efficiency of transporting EVRs from the BGS target to the mass analyzer is expected to be 20%, therefore the mass analyzer should be as efficient as possible. The target was set to  $> 95\%$  efficiency.
- Accept the emittance from the RFQ trap – The longitudinal emittance is expected to be  $15 \pi \cdot \text{mm} \cdot \text{mrad}$  and the transverse emittance is expected to be  $1 \pi \cdot \text{eV} \cdot \mu\text{s}$ .
- Ability to determine implantation time.
- Fit within existing space.

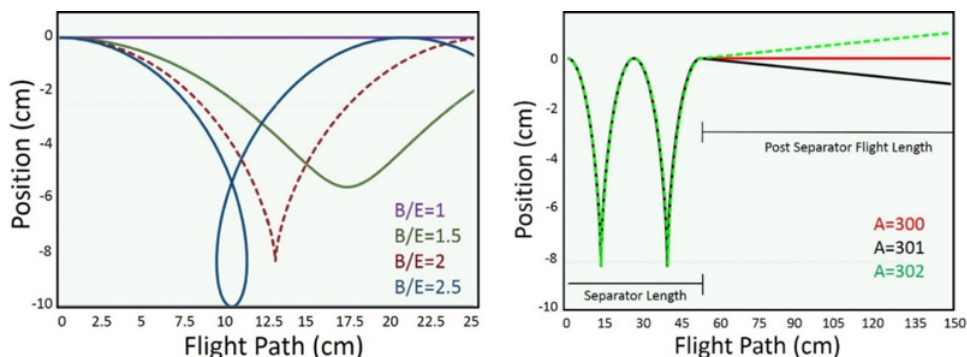


**Figure 3.** Trajectories of ions of  $A = 300\text{--}302$  in perpendicular  $E$  and  $B$  fields with  $B/E$  ratios of 1.0, 1.5, 2.0, and 2.5 (left) and trajectories of ions of  $A = 300\text{--}301$ ,  $q = 2+$  in and field with  $B/E = 2.0$  (right).

### 3.1 BGS + FIONA – Concept

Multiple different mass analyzers were simulated, including multi-reflection time-of-flight, Wien filter, and  $180\text{--}270^\circ$  bend magnet. However, none of these separators were capable of satisfying the requirements listed above. Therefore, we have designed a mass analyzer where particles are separated based on differing trochoidal trajectories in perpendicular electric and magnet fields.

Equations of motion for particles in perpendicular electric and magnetic fields are well known and can be found in references [21, 22], for example, and can be used for a first approximation of the separation principles. The projection of the path of a charged particle in perpendicular electric and magnetic fields is a trochoid in the plane perpendicular to the magnetic field. The equations of motion for a charged particle of mass  $m$  and charge  $Ze$  passing through a Wien filter with the electric field  $E$  and the magnetic field  $B$ , are given by:

$$x = a\omega t + \frac{v \sin(\theta)}{\omega} (1 - \cos(\omega t)) - \left( a - \frac{v \cos(\theta)}{\omega} \right) \sin(\omega t) \quad (1)$$

$$y = \frac{v \sin(\theta)}{\omega} \sin(\omega t) + \left( a - \frac{v \cos(\theta)}{\omega} \right) (1 - \cos(\omega t)). \quad (2)$$

Where  $v$  is the initial velocity in the  $x$ - $y$  plane perpendicular to the magnetic field,  $\theta$  is the angle between  $v$  and the  $x$ -axis, and  $\omega$  and  $a$  are defined by the relations  $\omega = ZeB/m$  and  $a = mE/ZeB^2$ . In a traditional Wien filter, the  $E$  and  $B$  fields are adjusted such that ions of a given velocity pass straight through the fields, which those of differing velocities are bent away. This is shown in Fig. 3 (left) by the line  $B/E = 1.0$ . However, if the magnetic field is raised relative to the  $E$  field, then the ions begin to take trochoidal trajectories through the field region. This is shown in Fig. 3 by the lines  $B/E = 1.5, 2.0$ , and  $2.5$ . The pitch of each trochoid is almost directly related to the  $A$  to charge,  $q$  ratio of the traversing ion. As such, it is possible to separate neighbouring isotopes based on their different  $A/q$  ratios, as shown in Fig. 3 (right).

To determine whether this separation principle would be suitable to differentiate between neighbouring SHE, simulations were performed with the charged particles simulation software *SIMION*<sup>®</sup>, version 8.1 [23]. *SIMION*<sup>®</sup> allows the user to construct three-dimensional representations of electrical elements and then the program calculates the electric

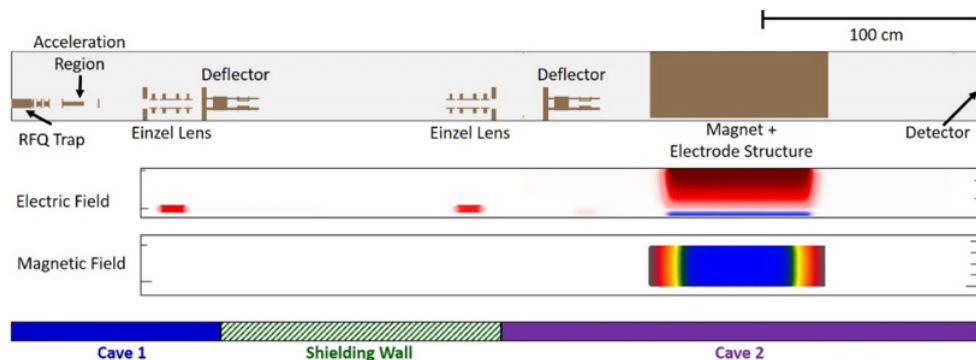


**Figure 4.** *SIMION*<sup>®</sup> representation of the FIONA setup (top), and the electric and magnetic fields observed by ions passing through FIONA (middle). Along the bottom is the physical location of the element at LBNL.

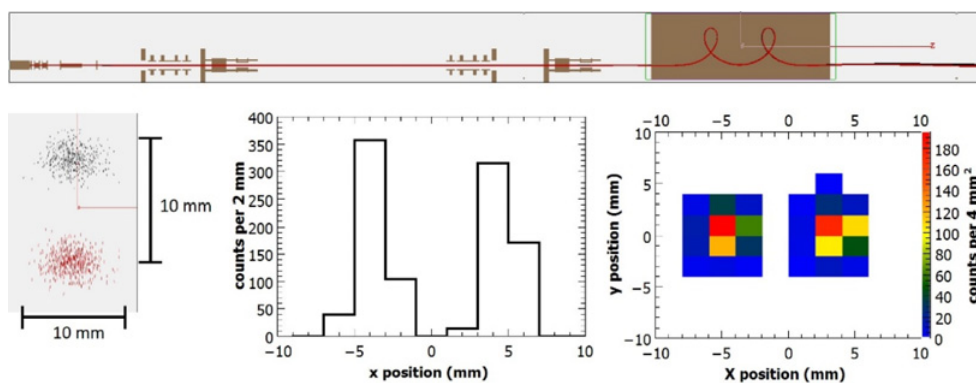


**Figure 5.** *SIMION*<sup>®</sup> simulations of ions with  $A = 288$  (red) and  $A = 289$  (black) and  $q = 2+$  through FIONA (top), expected distribution of ions reaching the FIONA focal plane (bottom left), with expected C3 pixelation (bottom right) and a two-dimensional projection of expected ion distribution in the C3 detector (bottom center).

fields around the element and the trajectories of charged particles through those elements. User programs can be added to include the effects of magnetic fields or gas on the charged particle trajectories. Figure 4 has an example of the simulation used to test the FIONA principle. The simulation includes an RFQ trap, acceleration region, two einzel lenses for beam focusing, two horizontal and vertical beam deflectors and an electrode structure inside a magnet to give perpendicular electric and magnetic fields. Figure 4 shows the equal potential lines for the electric and magnetic fields.

To determine the expected performance of FIONA, ions with  $A = 288$ – $289$  and  $q = 2+$  were cooled and trapped in a *SIMION*<sup>®</sup> RFQ trap, the trap was dumped, the ions were accelerated to energies of 5 keV and allowed to pass through the rest of the simulation and terminate in the C3 detector at the FIONA focal plane. The simulations were performed using  $B/E = 2.0$ . Figure 5 shows the trajectories of groups of 1000 ions of each mass, as well as the expected distribution of those ions on the C3 detector. The expected resolution is  $A/\Delta A \approx 1000$ , sufficient for SHE  $A$  determination. The simulated efficiency through FIONA was approximately 100%.

## 4. Conclusion and future outlook

FIONA is being installed at the focal plane of the BGS. Presently, the gas catcher, RFQ trap, acceleration region and magnet with an internal electrode structure have been installed. A control system for the beam line and the electronics has been developed and is being tested. Testing of the full apparatus is expected to begin in fall 2016. During experimental campaigns, the C3 detector will be placed at the focal plane of FIONA, allowing for detection of mass separated isotope and identification of photons emitted with those isotopes. This will open up a wide range of experimental studies at BGS + FIONA that will continue for the next decade.

## References

- [1] Yu.Ts. Oganessian and V.K. Utyonkov, Rep. Prog. Phys. **78**, 036301 (2015).
- [2] L. Stavsetra *et al.*, Phys. Rev. Lett. **103**, 132502 (2009).
- [3] Ch.E. Düllmann *et al.*, Phys. Rev. Lett. **104**, 252701 (2010).
- [4] J. Khuyagbaatar *et al.*, Phys. Rev. Lett. **112**, 172501 (2014).
- [5] S. Hofmann *et al.*, Eur. Phys. J. **A48**, 62 (2012).
- [6] D. Rudolph *et al.*, Phys. Rev. Lett. **111**, 112502 (2013).
- [7] J.M. Gates *et al.*, Phys. Rev. C **92**, 021301(R) (2015).
- [8] P.A. Ellison *et al.*, Phys. Rev. Lett. **105**, 182701 (2010).
- [9] Y.T. Oganessian *et al.*, Phys. Rev. C **70**, 064609 (2004).
- [10] Y.T. Oganessian *et al.*, Phys. Rev. C **69**, 054607 (2004).
- [11] Y.T. Oganessian *et al.*, Phys. Rev. C **74**, 044602 (2006).
- [12] P.J. Karol *et al.*, Pure Appl. Chem. **88**, 139 (2016).
- [13] P.J. Karol *et al.*, Pure Appl. Chem. **88**, 155 (2016).
- [14] K.E. Gregorich, Nucl. Instr. Meth. **A711**, 47 (2013).
- [15] J. Rissanen *et al.*, Phys. Rev. C **88**, 044313 (2013).
- [16] U. Forsberg *et al.*, Nucl. Phys. **A953**, 117 (2016).
- [17] Y.T. Oganessian *et al.*, Phys. Rev. C **87**, 014302 (2013).
- [18] G. Savard *et al.*, Hyperfine Int. **199**, 301 (2011).
- [19] J. Dilling *et al.*, Hyperfine Int. **127**, 491 (2000).
- [20] M. Block *et al.*, Eur. Phys. J. **A25**, 49 (2005).
- [21] W. Bleakney and J.A. Hipple, Phys. Rev. **53**, 521 (1938).
- [22] K. Yano and S.H. Be, Jpn. J. Appl. Phys. **19**, 1019 (1980).
- [23] D.A. Dahl, Int. J. Mass Spectrom. **200**, 3 (2000).